First publ. in: Physical Review B 56 (1996), 18, pp. 12242-12252

Excitations in a thin liquid ^{4}He film from inelastic neutron scattering

B. E. Clements*
Department of Physics, Texas A&M University, College Station, Texas 77843
and Institute Laue Langevin, 38042 Grenoble Cedex, France

H. Godfrin
Centre de Recherches sur les Tres Basses Temperatures, CNRS, Boîte Postale 166X, 38042 Grenoble, France

E. Krotscheck
Department of Physics, Texas A&M University, College Station, Texas 77843
and Institut für Theoretische Physik, Johannes Kepler Universität, A 4040 Linz, Austria

H. J. Lauter
Institute Laue Langevin, 38042 Grenoble Cedex, France

P. Leiderer
Fachbereich Physik, Universität Konstanz, Konstanz, Germany

V. Passiouk
Institute Laue Langevin, 38042 Grenoble Cedex, France
and Fachbereich Physik, Universität Konstanz, Konstanz, Germany

C. J. Tymczak†
Department of Physics, Texas A&M University, College Station, Texas 77843
(Received 5 September 1995; revised manuscript received 22 November 1995)

We perform a thorough analysis of the experimental dynamic structure function measured by inelastic neutron scattering for a low-temperature ($T=0.65$ K) four-layer liquid ^{4}He film. The results are interpreted in light of recent theoretical calculations of the (nonvortex) excitations in thin liquid Bose films. The experimental system consists of four outer liquid layers, adsorbed to two solid inner ^{4}He layers, which are themselves adsorbed to a graphite substrate. Relatively intense surface (ripplon) and bulklike modes are observed. The analysis of the experimental data gives strong evidence for still other modes and supports the long-standing theoretical predictions of layerlike modes (layer phonons) associated with excitations propagating primarily within the liquid layers comprising the film. The results of the analysis are consistent with the occurrence of level crossings between modes, and the existence of a layer modes for which the theory predicts will propagate in the vicinity of the solid-liquid interface. The theory and experiment agree on the detailed nature of the ripplon; its dispersion at low momenta, its fall off in intensity at intermediate momenta, and the level crossings at high momentum. Similar to experiment, the theory yields an intense mode in the maxon-roton region which is intrepreted as the formation of the bulklike excitation.

I. INTRODUCTION

Films of liquid helium adsorbed to solid substrates have been the subject of both theoretical and experimental studies for many years.[1] The interest in these systems is due to several facts: (a) in the film geometry more than in any other, the effects of the *short-range structure* of the quantum liquid, specifically the hard-core-like repulsion between individual atoms, becomes important. The adsorbate is, in the vicinity of the substrate, highly ordered in the form of individual atomic layers; (b) modern theoretical analytic[2] and computational[3] tools are today sufficently refined and efficient that a quantitative microscopic analysis of the ground-state structure is feasible for these systems. There is little need to implement hard to control phenomenological input other that the underlying microscopic Hamiltonian; and (c) experimental techniques are sensitive enough to reveal direct evidence for the microscopic, short-range structure of these systems.

A full understanding of the low-temperature thermodynamic properties of ^{4}He films begins with a thorough investigation of their structural and dynamical properties. Concerning the *structural* properties, a primary issue is how the microscopic correlations, stemming from atom-atom and atom-substrate interactions, will inevitably determine the various structural phases of solid-layer films, or the layering which occurs in thin liquid films. Elastic neutron scattering has provided an excellent experimental method for determining the structural phases of solid ^{4}He films.[4] In the case of the *dynamical properties*, one is again concerned with how the microscopic correlations will influence the excited-state properties of the film system. Here, considerable work has been focused on liquid films — as well, it is the concern of the present work.

Our goal is to fully analyze inelastic neutron scattering data, for a four-layer liquid film, obtained at the Institut Laue-Langevin. An accompanying theoretical paper[5] complements this analysis by providing a theoretical basis for interpreting the results. We defer a more detailed discussion of the experimental system until Sec. III, for now it suffices to highlight the general characteristics of the film system. The ^{4}He film was absorbed on a graphite substrate and the temperature was held at approximately 0.65 K throughout the scattering experiment. When dealing with graphite, a word of caution is in order since it is well established that the first two layers of helium, adjacent to the graphite, are frozen at sufficiently low temperatures. The total surface coverage of these two layers is determined from elastic neutron scattering[4] to be 0.2 Å^{-2}. We speak of these two layers as being inert, and all future discussions of the film's coverage will refer to the liquid layers only. Consequently, the four-layer film under consideration consists of six layers of helium; two are frozen, three are nearly completed liquid layers, and the fourth liquid layer is partially complete. To a high degree (but unfortunately, not total) the scattering contributions coming from the liquid layers and the solid bilayer-substrate can be distinguished from each other. Further discussion of this point will be made in Sec. V.

Well below a temperature of 1 K, a four-layer ^{4}He film is in a good regime to probe the dynamical excitations of interest for the following reasons. First, vortex excitations are of no direct concern since the Kosterlitz-Thouless transition is well above 1 K for this coverage.[6] Second, 0.65 K is well below the melting temperature[7] of the second solid layer which occurs at approximately 2 K. Third, at this coverage we are still in the thin film regime. At somewhat higher coverages, the bulk and surface modes dominate the measured scattering signal. As discussed below, this reduces the chances of detecting other modes associated with thin films. In spite of this there is enough ^{4}He present to allow a quantitative data analysis to be carried out. For smaller and smaller coverages it becomes increasingly difficult to discern the physical modes from fluctuations in the scattering signal.

Significant experimental and theoretical progress has led to an increased understanding of the excitations in ^{4}He films. It is not our intent to summarize these studies here, rather we only consider some aspects directly relevant to the present analysis. For thick films, e.g., 100 atomic layers, a bulk phonon-maxon-roton mode and a surface mode are the main excitations. Studies of these modes date back approximately 40 years.[8]

For thin films, ideally less than 6 or 7 layers thick, the visible (nonvortex) excitations are more numerous in variety. Surface modes propagating at the liquid-gas interface are still present, and depending on whether they are driven by restoring forces due to the substrate-helium interaction (or gravity) or the interfacial surface tension, they are referred to as third sound and ripplons, respectively. These modes were first measured, up to relatively large wave vectors, in neutron scattering experiments carried out at the Institute Laue-Langevin.[9–12] Above a certain coverage a ''bulklike'' mode develops that will eventually become the bulk phonon-maxon-roton curve. Experimentally, already by three layers a precursor to the bulk mode is strikingly present. It is important to note that in neutron-scattering experiments there is a chance that this quasibulk mode will form prematurely because of capillary condensation; helium tends to pool at the boundaries of the crystallites making up the substrate. While there was a period of time when it was thought that these two modes are the predominant ones, theoretical calculations soon showed that other modes should also be present,[13] and their spectral strength should be significant. These earlier works have been followed by many others.[14–21] It was soon determined that the highly layered nature of the liquid film[2] allowed certain of these new modes to be identified as propagating within individual layers.[22–24] The modes were termed ''layer phonons.''

The outline of the paper is as follows. In Sec. II we give a brief review of theoretical results, and present a qualitative overview of the general characteristics of the various modes. We will consider two calculations for the film's dynamic structure function: a generalized Feynman theory and a theory which includes three-phonon scattering processes. The theoretical details are omitted; we leave the interested reader to consult Ref. 22 for earlier work, and the accompanying paper[5] for the most complete first-principles calculation done to date. A discussion of the neutron scattering experiment follows in Sec. III. The analysis of the neutron-scattering experiment is presented in Sec. IV. There, we will argue that an assortment of modes are in fact seen experimentally. Finally in Sec. V, the results of the data analysis and theoretical considerations are combined in a discussion. Concluding remarks are given in Sec. VI.

II. EXPOSÉ OF THEORETICALLY DETERMINED EXCITATIONS

In the neutron-scattering experiments described below, the Born approximation provides the key relation between the measured differential scattering cross section and the dynamic structure function $S(\mathbf{k},\omega)$:

$$\frac{d^2\sigma}{d\Omega\, d\omega} = \frac{k_f}{k_i}\left(\frac{d\sigma}{d\Omega}\right)_0 S(\mathbf{k},\omega), \tag{2.1}$$

where $(d\sigma/d\Omega)_0$ is the differential scattering cross section for scattering from a single constituent, and $\mathbf{k}_i$ and $\mathbf{k}_f$ are the initial and final momenta, $\mathbf{k}=\mathbf{k}_f-\mathbf{k}_i$ and ω are the momentum and energy transferred to the system by the neutron. The calculation of $S(\mathbf{k},\omega)$ requires knowledge of both the excitation spectrum E_n-E_0 and the complete set of transition densities $\langle\Psi_n|\rho(\mathbf{k})|\Psi_0\rangle$; as can be seen from the expression

$$S(\mathbf{k},\omega)=\sum_{n\neq 0}|\langle\Psi_n|\rho(\mathbf{k})|\Psi_0\rangle|^2\,\delta(\hbar\omega-E_n+E_0). \tag{2.2}$$

The zeros in this expression signify the ground state, and the operator $\rho(\mathbf{k})$ is the density operator. In the experimental situation, the scattering is done at approximately grazing angles relative to the basal planes of the graphite substrate. To conform to this geometry a dynamic structure function $S(q_\parallel,\omega)$, is calculated in the theory, where the relevant momentum, $q_\parallel$, now lies *exactly* parallel to the substrate. Since true grazing angle scattering in the experiment is an idealization (due to powder contributions and nonplanar orientations of the crystallites making up the scattering sample) we will distinguish the experimental momentum transfer from

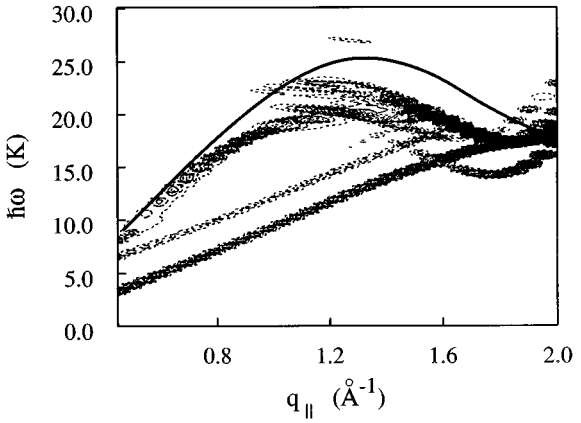

FIG. 1. The theoretical dynamic structure function calculated from the Feynman theory of excitations, generalized to the film geometry. The intensity of the mode is reflected in the shade of the grayscale. The solid curve is the bulk phonon-maxon-curve calculated in the bulk Feynman theory. The lowest energy excitation, at small $q_\parallel$, is the surface ripplon; the highest energy modes below $q_\parallel = 1.8$ Å^{-1}, are layer modes; and the modes occurring between these are the intermediate modes referred to in the text. The most intense layer mode will develop into the bulk phonon-maxon roton.

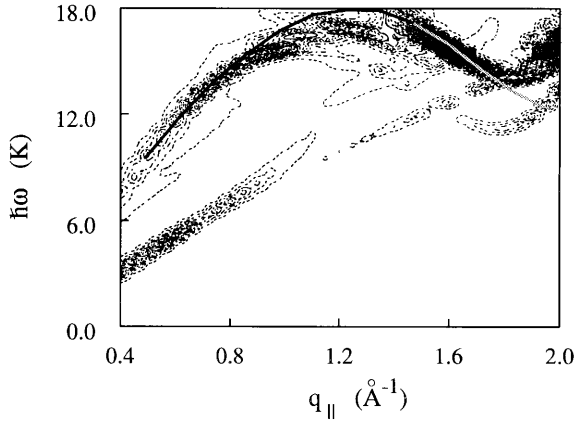

FIG. 2. The same as Fig. 1, but with three-phonon scattering processes included. The solid curve is the corresponding bulk mode, determined at the same level approximation. The lowest energy mode, at small $q_\parallel$, is again the surface ripplon. The intermediate mode has been highly damped by the three-phonon scattering processes. The high energy modes, are again layer modes, but the bulk mode is apparently enhanced over that of the Feynman theory.

the theoretical $q_\parallel$ by denoting it by k. Further discussion of the theory related to these aspects can be found in Ref. 22.

A good starting calculation for $S(q_\parallel,\omega)$ in the films is to use the Feynman theory of excitations[25] (generalized to the inhomogeneous geometry[26]), where the elementary excitations are described by the ground state being modified by single density fluctuations.[22] Experience has shown that in spite of quantitative deficiencies, the qualitative features of the model are quite satisfactory. Moreover, for purposes of viewing the modes, the Feynman calculation is sometimes preferred since mode damping occurring in more refined theories[5] has the obvious (correct) effect of mode broadening and hence reducing the visibility of certain modes. In Fig. 1 we show $S(q_\parallel,\omega)$, calculated using Feynman theory for a four-layer film ($n = 0.240$ Å^{-2}). In this and the following contour plots, the most intense modes have been reduced to enhance the visibility of the weaker modes. For a one-to-one comparison with experiment, we have limited the momentum in the figure to the accessible domain of our data analysis. In the theory, transition densities and the one-body currents are used to reveal the regions of the film where a given mode propagates (for a given momentum) and its physical nature.[22]

For $q_\parallel$ below 1.5 Å^{-1}, the lowest energy mode in Fig. 1 is a ripplon propagating in the vicinity of the liquid-vapor interface. In this momentum range it has a highly linear dispersion relation. This observation implies that multiphonon processes will have a smaller effect than otherwise, in renormalizing this mode — to a high degree the mode will maintain its present dispersion even in more sophisticated calculations.[5] At very high energies a mode has started to develop that has the characteristic maxon-roton shape, although at the Feynman level the coverage is still too low since the maxon has only started to form. Immediately below this a second, and fragments of a third, phonon-maxon-roton curve are visible. To the extent that these modes can be clearly identified, they correspond mostly to excitations propagating in individual layers. They have been termed ''layer phonons,'' where the term phonon generically represents any layer phonon-maxon-roton-type excitation with predominantly longitudinal polarization. We note here that the complication in identifying the nature of the modes increases with increasing energy. At high energy, the Feynman wave function(s) characterizing a mode has many oscillations with nodes distributed over space and thus a clear identification becomes increasingly difficult.

Between these modes there is second mode with dispersion resembling the ripplon, but with less strength. At $q_\parallel = 1.6$ Å^{-1} there is a distinct level crossing of the ripplon and the lower-energy layer maxon roton. Since the two modes propagate in different locations of the film, the modes distort very little as they cross. Above $q_\parallel = 1.6$ Å^{-1} the lowest energy mode is a layer roton propagating in the first liquid layer of the film (at the solid-liquid interface). Near $q_\parallel = 1.8$ Å^{-1} the ripplon again crosses with the quasibulk mode, and in the process moves to higher energy and is reduced in strength.

Three-phonon scattering processes have also been included in the calculation of the dynamic structure function[5] in the film system. In Ref. 5 this approximation is given the abbreviation CBF-BW. While the term three-phonon is common in the literature, it is again somewhat misleading since the scattering can be between a phonon and ripplon, for example. By in large, three-phonon processes do not change the results significantly from those obtained using the Feynman approximation. In Fig. 2, $S(q_\parallel,\omega)$, calculated within this approximation, is shown for the same coverage of $n = 0.240$ Å^{-2}. The inclusion of three-phonon processes does lead to a few notable differences such as a lowering of the energy of the layer-phonon modes by a significant amount in the intermediate momentum regime. This is expected since the analogous situation occurs in bulk ^{4}He, where three-phonon processes lower the calculated roton minimum by 25%. As commented above, the energy of the

surface mode is hardly changed by the three-phonon scattering. Interestingly, however, there is a substantial reduction in its intensity for momenta above $q_{\parallel}=0.8$ Å^{-1}. As in the Feynman approximation the surface mode level crosses with the layer-phonon modes at large momentum. After including three-phonon effects (thus giving the modes a means to decay by mode splitting) modes above a certain threshold energy are broadened and the linewidth indicates the inverse lifetime of the mode. As a result of this broadening the nearly linear mode between the ripplon and the layer phonons is damped to the point where the contours only show a small portion of it. Nevertheless, the presence of the mode enhances the broad low-intensity ''background'' contribution to the scattering intensity.

One final change, occurring by including three-phonon contributions, is that the maxon-roton region of the quasibulk layer phonon is enhanced. This is immediately apparent from the figures, and further supported by the solid curves in these figures. For the respective approximations, the solid curves are the 3D bulk modes at a density of 0.022 Å^{-3}. This is an interesting observation for the following reason. In the experimentally measured $S(k,\omega)$, one observes a ''prematurely'' formed bulklike phonon-maxon-roton curve, in the sense that it resembles a bulk mode that, according to the Feynman theory, is expected for much thicker films. The accepted explanation for this was that capillary condensation at the borders of the graphite crystallites is responsible for the presence of a bulklike mode even though the majority of the crystallites are covered with much less ^{4}He. The theoretical finding that an enhancement of the roton maxon can arise simply by including three-phonon processes in $S(k,\omega)$ certainly weakens the need to introduce capillary condensation to explain this phenomena.

Finally, we mention that in Ref. 5 another approximation is presented and discussed, which takes into account the fact that the intermediate states in the three-phonon processes should be renormalized by further self-energy corrections. This is achieved by multiplying the Feynman excitations, that occur in the energy denominator of the CBF-BW expression, by a single scaling parameter which is adjusted to make the spectrum agree with the experimental one in the bulk limit. As a result of that improvement, one achieves near quantitative agreement between the theory and experiment for both the energy and location of the roton minimum, and for the static response function. Because this calculation does not alter the types of excitations, we will not discuss it further here. However, the dynamic structure function obtained in that approximation will be contrasted to the experimental one in the final sections of this paper.

III. EXPERIMENTAL BACKGROUND

Helium was adsorbed onto a substrate of exfoliated graphite (Papyex[27]). Besides having a powder contribution, Papyex has oriented graphite crystallites having a 30° (FWHM) mosaic distribution with respect to the c axis. The sample was mounted with the c axis perpendicular to the scattering plane. For the experimental run that generated the data analyzed here, the system was held at a temperature of 0.65 K. Experiments were carried out at several other temperatures but the results will not be analyzed here for reasons explained below. Spectra obtained from the sample cell before any ^{4}He was adsorbed were used as background and subtracted from the spectra of subsequent measurements with adsorbed ^{4}He.

The first layer of helium, under the pressure of the second layer, had an areal density[28] of 0.115 Å^{-2}. It consisted of 312 cc (STP) of ^{4}He. The average coherence length deduced from the diffraction peak of the first layer was 300 Å. This gives the average size of the graphite crystallites. The second layer had a density of 0.095 Å^{-2}, and subsequent layers were taken to have areal densities of 0.078 Å^{-2}. Using these values, one can convert from coverages to layers. The film analyzed here had a liquid layer coverage of 0.239 Å^{-2} which, by using 0.078 Å^{-2} per layer, translates into slightly more than three-completed layers. It is important to note that the coverage of the outer layer, estimated by this means, has a fairly large uncertainity. In Ref. 5 the theoretically determined density profile for the film is shown. There it is evident that the fourth layer of a film with total coverage 0.240 Å^{-2} is closer to being half complete. This implies that the film is probably too thin for the standard conversion factor (0.078 Å^{-2} per layer) to be reliable.

The inelastic neutron-scattering experiments were performed on the time-of-flight spectrometer IN6 at the ILL with an incident wavelength of 5.12 Å. The detectors were located in an angular range that correspond, for elastically scattered neutrons, to momentum transfers between 0.254 Å^{-1} and 2.046 Å^{-1}. The energy resolution depended only slightly on the momentum transfer; a good estimate of it is 0.6 – 0.7 K.

The dynamic structure function is typically expressed as a function of the momentum k and energy $\hbar\omega$ transferred to the system from scattered neutron. Technically, however, the experimental scattering function is not measured along lines of constant k but rather along lines of constant scattering angle ϕ, subtending the incident and final momenta in Eq. (2.1). Along the elastic line ($\hbar\omega=0$) the corresponding momentum k_e, and ϕ are simply related: $k_e=2k_i\sin(\phi/2)$, where the incident momentum $k_i=1.227$ Å^{-1}, corresponding to the incident wavelength, is fixed in the experiment. Off the elastic line the relation between these two quantities is $\hbar\omega$ dependent but in the energy-momentum regime where the scattering intensity in the films is significant, constant ϕ and constant k maps are nearly identical. Consequently, in the figures below, the momemtum variable stated is the elastic momentum.

IV. ANALYSIS OF EXPERIMENTAL RESULTS

In this section we present our analysis for the scattering data measured in the experiment. The experimental dynamic structure function for the four-layer film is shown in Fig. 3. Each horizontal line is at a different momentum, the lowest and highest being 0.25 Å^{-1} and 2.05 Å^{-1}, respectively. Two modes are most apparent. The low-energy, low-momentum mode is a ripplon, and the other (higher-energy) mode with significant weight is the ''bulk-like'' phonon-maxon roton, mentioned previously. To a good approximation, although not completely,[11] this mode has dispersion roughly agreeing with the experimental bulk mode at saturated vapor pressure; it has a roton gap of *approximately* 8.6 K, for example. For energies below that of the ripplon, and at low momentum,

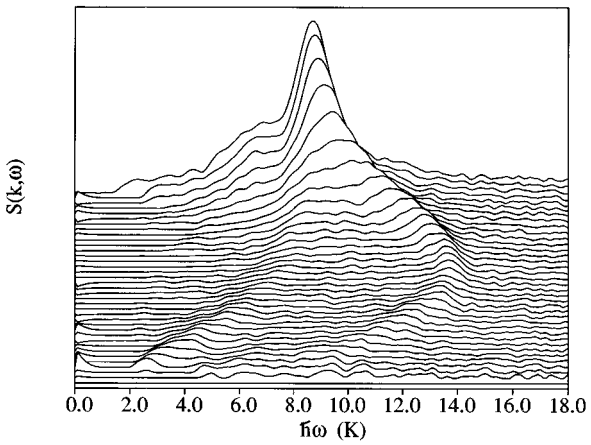

FIG. 3. Experimental dynamic structure function determined for a four-layer liquid film ($n=0.239$ Å^{-2}), at $T=0.65$ K. Each curve represents a different momentum, with the lowest and highest being $k=0.25$ Å^{-1} and $k=2.05$ Å^{-1}, respectively.

little scattering takes place. Above the bulklike phonon-maxon roton, a uniform background of scattering intensity is evident and arises from multiphonon processes. Between the phonon-maxon-roton excitation and the ripplon, there is a plateau in the scattering intensity. To make further progress we quantitatively investigated the scattering function. This was done by attempting to fit the true modes with Gaussians, and the background with a smooth polynomial. In doing so, we found that some of the above statements must be modified. We now summarize our analysis and then proceed to the actual results.

The determination of the *best fit* of $S(k,\omega)$ for a fixed k began first by attempting to *define* the multiphonon background. The next step was to simultaneously vary the number of Gaussians and their linewidths. After it was decided that the appropriate number of Gaussians were found, our fitting algorithms were given full liberty to determine the best fit parameters (the locations of the Gaussians, their strengths and linewidths, and the background polynomial). An additional important criterion for the overall best fit was that continuity in the fitting parameters must be preserved when going from one fixed k scan to the next. This procedure was repeated many times in search of the best possible fit to the data.

We had two important guides for choosing the background to be a smooth polynomial.

(i) First, our theoretical work on films in Ref. 5 shows that if three-phonon processes can be taken as representitive, then for energies and momentum of interest here, the background is quite structureless. In fact from the zero-temperature theory, most of the *apparent* background comes from the superposition of the tails of the lines shapes of the true modes. Due to the large instrumental resolution, this effect is even bigger in the experimental case but it must be stressed that this is *not* the contribution to the background referred to in our data analysis. Rather, the background is the total scattering function minus the Gaussian contributions. It is precisely these subtracted contributions that are found to be small and structureless in the theory.

In this context, it is interesting to contrast the film to the bulk system. In the bulk case there is non-negligible scattering (structure) observed at energies approximately equal to twice the roton energy and also at energies equal to the sum of the roton and the maxon energy. The well-known[29] origin of this scattering is from large contributions to the two-particle density of states (DOS) coming from the single-particle DOS of the roton and the maxon. In the film the situation is different. Only at very low coverage, where a single mode carries most of the strength, is the analogous scattering observed. For thicker films, the large number of modes having gradual dispersion (and thus a large DOS) apparently smears out this effect to the point where it contributes no distinct structure at the energies and momentum of interest here.

(ii) Second, although not reported here due to complications in the analysis, we also examined, on a qualitative level, experimental neutron-scattering data for temperatures above 1 K. Observing the temperature variations of the $S(k,\omega)$ provided a useful tool for identifying multiphonon effects. This was especially useful in understanding the scattering that was observed in the experiment at energies below the ripplon and the layer roton. Invoking our three-phonon theory, energy and momentum conservation at zero temperature says that there should be no multiphonon scattering below these modes. Consequently, the question arises to whither that should be true at a temperature of 0.65 K. By rough comparison of the runs done at different temperatures, we concluded that that scattering intensity in that low-energy region is highly temperature dependent and would probably not survive an extrapolation to zero temperature. Thus, the scattering in this region was associated with multiphonon effects and not true modes. This conclusion may appear to be inconsistent with low-temperature bulk studies but we hasten to point out that the scattering strength of concern here is many orders of magnitude less than the scattering strength in the bulk studies. For example, $S(k,\omega)$ for the bulk roton in our full cell experiment was $4-5$ orders of magnitude stronger in intensity than the scattering strength in this region. Consequently, such a small amount of scattering will easily go unnoticed in a bulk experiment.

Our conclusions of this study are that (i) a smooth polynomial is satisfactory and (ii) that the parameters of the polynomial could be determined by fitting the magnitude and the slope of the high-energy data above the quasibulk mode, and the low-energy data below the ripplon and layered mode.

Separate trial fits with three, four, and five Gaussians were tested. The theory shows that one should not expect the number of Gaussians to be constant for a given coverage, but rather certain modes only have significant strength at higher momentum. This consideration was taken into account when we analyzed the data; specific details will be given in the discussion below.

Determining the proper linewidth for the Gaussian fit functions was also an important task. An extensive number of different widths were sampled, but in the final analysis only linewidths close to the experimental instrument resolution were taken as reasonable. The primary guide for choosing acceptable linewidths came by fitting the two prominent modes — the ripplon and the bulklike mode. Mild linewidth variations arose when the fitting functions were made to comply with these modes as they varied from one point in $(k,\hbar\omega)$ space to another. This gave the linewidths a slight

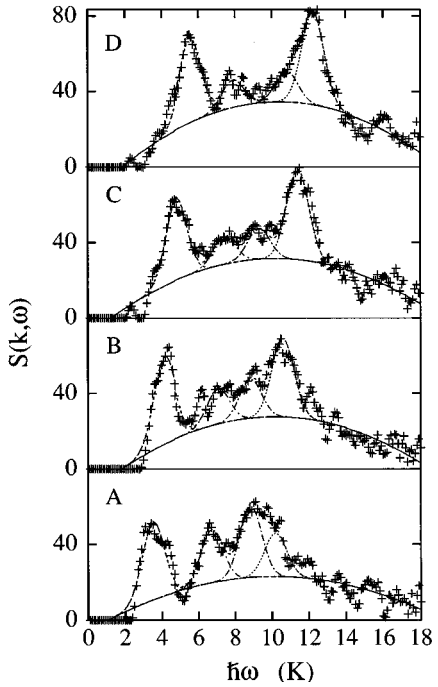

FIG. 4. Low momentum $S(k,\omega)$ for (a) $k=0.50$ Å^{-1}, (b) $k=0.60$ Å^{-1}, (c) $k=0.70$ Å^{-1}, and (d) $k=0.80$ Å^{-1}. The + symbols are the raw data, the solid and broken curves are fits to the multiphonon background and the physical modes. The sum of the background and Gaussians is also shown in each plot, although usually hidden by the data points.

(but generally well-known) momentum dependence; regions where the dispersion curve is relatively flat (the maxon and roton being the well-known examples in the bulk experiments) will have slightly larger measured linewidths, for example. The only working hypothesis available to us, which we believe is nevertheless the only reasonable one, was to assume that a good fit of the prominent modes implied that we could use the similar linewidths for the less pronounced modes. The theory gave no reason for assuming otherwise; no calculated modes have a linewidth nearly as large as the instrumental resolution. We assert that this approach produces an overall good fit — when the lesser intensity modes protrude out of the background plateau they are typically fit quite well by this procedure. Note also and as expected, these linewidths provide a correspondingly good fit to the full cell phonon-maxon roton. This concludes our summary of the analysis but before proceeding to the details, we stress that to within reasonable variations of parameters, the representive fit discussed now (and shown in the figures) is quite robust for the ripplon and bulklike mode at all momenta. For momentum above 1.4 Å^{-1} the fit is believed to be equally reliable for all the modes, given that the background polynomial is the appropriate one (again, to within reasonable variations).

Figures 4–8 show $S(k,\omega)$ for fixed k. In each figure we show the raw experimental data; a (second-order) polynomial fit to the multiphonon background; and a set of Gaussians, with linewidths set at approximately the experimental resolution of the detector. The sum of the contributions from the Gaussians and the background polynomial is also plotted in each figure, but in most cases it is hidden by the experimental points, indicating the overall quality of the fit. As discussed, during the fitting procedure the Gaussian strength and location, and the polynomial trial functions were varied simultaneously to achieve the overall best fit.

We now consider our results. Since the strength of the majority of the modes increases with k (with the ripplon being the important exception) the logical progression for our discussion is to start at high k and work backwards. From the experimental viewpoint, Fig. 6(d), and Figs. 7 and 8, are the most significant ones in this paper — as we will see momentarily, they support for the first time, rather unambiguously, the existence of modes that undergo level crossing in thin ^{4}He films. In these figures each $S(k,\omega)$ is fit with either four or five Gaussians, each with non-negligible strength. At $k=2.05$ Å^{-1} five Gaussians are need to achieve a good fit to the data. The background provides a nearly flat contribution to the overall intensity. One Gaussian totally consumes the central peak which has the energy of the bulk roton. Four less intense Gaussians flank that, and form the observed shoulders in the data. The HWHH is approximately the experimental instrument resolution for each Gaussian. At $\hbar\omega\approx 0$, the observed intensity jump arises from the graphite Bragg peak, and is not related to the liquid film. The background polynomial encompasses the very low energy lip in the range, 2 K $\leqslant\hbar\omega\leqslant$ 4 K. As stated above, our confidence that this lip should be associated with the multiphonon background, and not a real mode, comes by studying the temperature dependence of $S(k,\omega)$. Parenthetically, a full quantitative analysis, similar to the one we give now, was not possible at elevated temperatures that were also probed during the experiment, thus we refrain from anything other than qualitative statements. By focusing on the experimental $S(k,\omega)$ for energies between 0 K $\leqslant\hbar\omega\leqslant$ 6 K, in the vicinity of $k=2$ Å^{-1}, it is clear that the lip is highly temperature dependent; at higher and higher temperature the lip extends

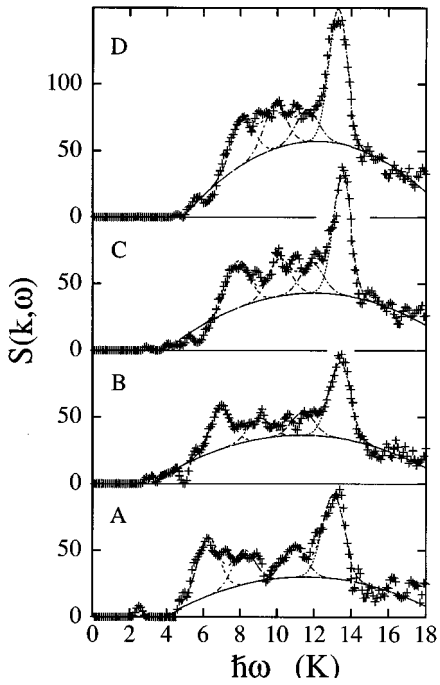

FIG. 5. Same as Fig. 4, with momentum (a) $k=0.95$ Å^{-1}, (b) $k=1.10$ Å^{-1}, (c) $k=1.30$ Å^{-1}, and (d) $k=1.40$ Å^{-1}.

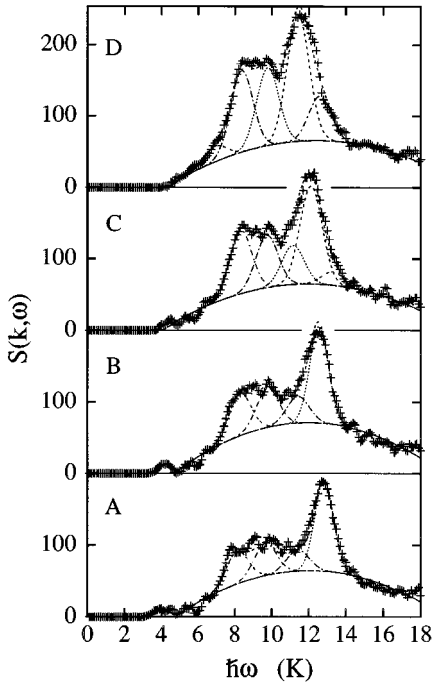

FIG. 6. Same as Fig. 4, with momentum (a) $k=1.50$ Å^{-1}, (b) $k=1.55$ Å^{-1}, (c) $k=1.60$ Å^{-1}, and (d) $k=1.65$ Å^{-1}.

to lower and lower $\hbar\omega$. Indeed, it is reasonable to believe that the lip will nearly vanish at zero temperature, up to $\hbar\omega\approx 4$ K. In this way, we reason that the lip should be associated with the background. In fact the lowest mode fitted with a Gaussian is very weak and not without suspicion, for the same reason. Proof that this is likely to be a real mode comes from the observation that its intensity is significant over a range of momenta. On the other hand, the mode between 5 K $\leqslant\hbar\omega\leqslant$ 8 K is quite resilient to changes in the temperature, i.e., at $T=0.65$ K, its intensity profile is not expected to differ appreciably from that of $T=0$.

Proceeding to smaller k, the next observation of importance is made at $k=1.95$ Å^{-1}, where the primary peak in the data is broadened beyond the width where a single Gaussian will consume the total intensity. This is a sign that the acclaimed bulklike mode is not a single mode for all k, but rather comes from a contribution of several modes. For discussion purposes it is convenient to tag this large intensity mode with a label; we will refer to it as the primary mode. Decreasing k further one finds, in the momentum range 1.70 Å$^{-1}\leqslant k\leqslant 1.75$ Å^{-1}, that the primary mode can no longer be distinguished from its neighbors. To make further progress in sorting out the various modes we must proceed to lower k.

The small intensity maximum at approximately 11 K in Fig. 7(a), is important as can be seen from Fig. 6, where the same mode has considerably more strength. We can now attempt to put these observations into perspective by jumping to low momentum and observing how the primary mode evolves as k increases. We propose that at $k=1.50$ Å^{-1} the high energy, intense mode is the primary mode. Near $k=1.55$ Å^{-1} it begins to level cross with a second, less intense mode. At $k=1.60$ Å^{-1} it continues to cross. Note that the extremely low strength mode at $\hbar\omega\approx 13.5$ K, is *not* believed to be significant. Finally, at $k=1.65$ Å^{-1}, the primary mode has completed the level crossing. In light of this trend we now return to Fig. 7(a) to see that the natural explanation for the Gaussians in this figure is that the primary mode level crosses for a second time with yet another mode. There it maintains its position relative to the other modes, up to at least $k=2.05$ Å^{-1}.

One must not lose sight of the fact that the above discussion is nothing more than an interpretation to the fits of the experimental data. Credibility to this interpretation can be

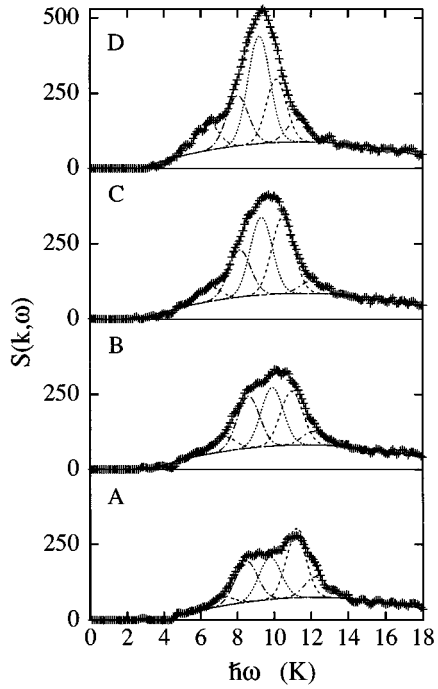

FIG. 7. Same as Fig. 4, with momentum (a) $k=1.70$ Å^{-1}, (b) $k=1.75$ Å^{-1}, (c) $k=1.80$ Å^{-1}, and (d) $k=1.85$ Å^{-1}.

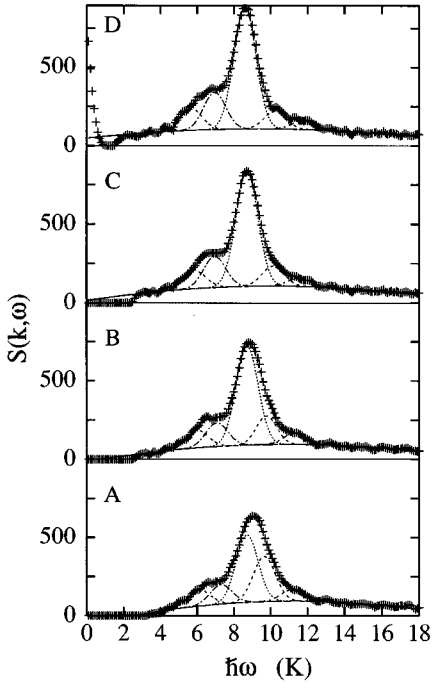

FIG. 8. Same as Fig. 4, with momentum (a) $k=1.90$ Å^{-1}, (b) $k=1.95$ Å^{-1}, (c) $k=2.00$ Å^{-1}, and (d) $k=2.05$ Å^{-1}.

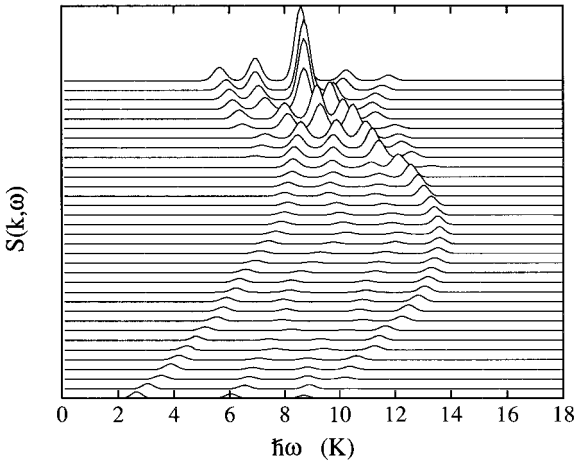

FIG. 9. The dynamic structure function constructed from the Gaussian fit functions. The background function has been subtracted out and the Gaussian widths have been narrowed to enhance the visibility of the modes.

gained in two ways. The first is that the scenario agrees well with theoretical calculations (Sec. V and Ref. 5). The second is by looking at the entire $S(k,\omega)$ constructed from the Gaussian fits. This is done in Fig. 9; the corresponding contour plot is shown in Fig. 10. In these plots the background polynomial is subtracted out, and the Gaussian widths are artifically reduced to enhance the mode visibility. Especially from the contour plot, one achieves the impression that the primary mode does exhibit the above described level crossings.

We have also included in the figure, the SVP bulk mode for comparison (the solid curve). It is clear that the primary mode is the developing bulk phonon-maxon-roton mode, but as already pointed out in previous work,[11] the maxon has slightly less energy than the experimental bulk maxon; even for lower coverage films the maxon's energy is a feature in the data that can be accurately followed. As discussed in Ref. 11, the maxon gains energy with increasing coverage for these lower coverage films. This further supports our statement that we are still in a coverage regime where this mode is most appropriately classified as being the *precursor* to the bulk mode. Equivalently, the less intense modes flanking the *quasibulk* mode are not negligible in the maxon-roton regime.

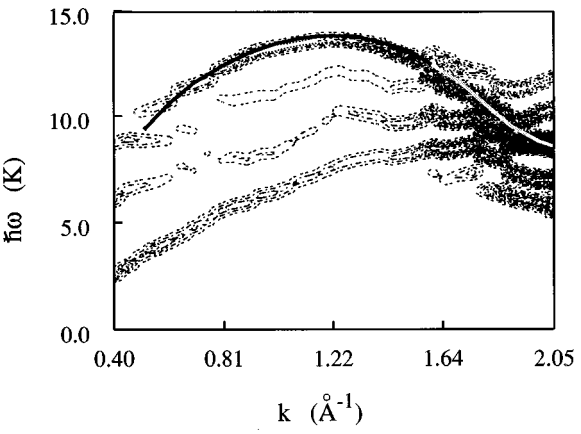

FIG. 10. A contour plot representation of the $S(k,\omega)$ in Fig. 9. The solid curve is the experimental SVP bulk phonon-maxon-roton curve superimposed on the contour plot. For momentum below $k=1.60$ Å^{-1} the lowest energy mode is the ripplon. (See text for further discussion.)

We now return to the low and intermediate momentum regimes. Here, because of substantial fluctuations in the experimental data, the actual fitting procedure was more difficult and more uncertain. Obtaining a fit completely free of doubt was not possible. For example, forcing five Gaussians produced artificial distortion in the overall fits in the ripplon and maxon. On the other hand, four Gaussians produce the rather strange mode-kink observed near $k=1.2$ Å^{-1}. The relevant figures are Figs. 4 and 5. We will provide two speculative reasons for this in the next section, but a complete answer will require further experimentation. Two facts, however, do remain unchanged by the various attempted trial fitting functions, and these will now be commented on. Our first observation is that the ripplon, which was measured successfully down to $k=0.25$ Å^{-1}, is easily followed below $k=1.0$ Å^{-1} but loses intensity for higher k. The second is that in this momentum range there is little doubt that modes exist other than the ripplon and quasibulk mode. Note that in Figs. 4 and 5 the lowest (highest) energy mode is the ripplon (quasibulk mode). The Gaussians between these two modes are the modes that we are referring to.

V. EXPERIMENT AND THEORY COMPARISON

Finally, we are in a position to compare the experimental fitted data with the theoretical $S(q_{\|},\omega)$. Already several comments above have been made in this regard but they will be summarized here for completeness. We follow the outline where we first discuss the ripplon; second, the intermediate energy modes; and third, the quasibulk mode. For the most part, Figs. 2 and 10 are the relevant ones in the following discussion. An analogous discussion that is slanted towards the theoretical side can be found in Ref. 5.

The qualitative and semiquantitative agreement between the experimental and theoretical ripplons is the following, in both cases.

(i) There is a small but obvious energy gap between the higher energy modes and the ripplon at very long wavelengths (not shown in the figures). The longest wavelength probed experimentally had momentum $k=0.25$ Å^{-1}.

(ii) At low momentum the ripplon has significant strength but loses much of that strength in the vicinity of $k=1.0$ Å^{-1}.

(iii) The ripplon level crosses twice, first with the lowest energy layer-maxon roton, and second with the developing bulk mode. It then continues to high energies. This interpretation of the data comes from the theoretical analysis by studying the transition densities and the one-body currents. There it seen that the nature of the mode at $\hbar\omega \approx$ 18 K, and $k=2.0$ Å^{-1}, in Fig. 2, is the same as the low energy ripplon.

From Figs. 4–8, there is little doubt that intermediate energy modes exist between the ripplon and the quasibulk mode in true liquid ^{4}He films. As stated numerous times, this is in complete agreement with theory. A semiquantitative comparison in the range of $k \leqslant 1.5$ Å^{-1} and intermediate energies, is hampered somewhat by the fact that the experimen-

tal and theoretical modes are weak. In the theoretical plot, Fig. 2, the remanents of a mode are still seen, especially near $k=1.3$ Å^{-1} and $\hbar\omega = 12$ K. Unfortunately, the contour plot gives slightly the wrong impression since it looks as though the ripplon at $k=1.1$ Å^{-1} is pointing towards the high energy finger of this mode near 12 K. However, from the current and transition densities it is easily verified that the mode in the vicinity of 9 to 10 K is the true continuation of the ripplon.

In the experiment (see Fig. 10) two intermediate energy modes have been followed by the fitting analysis. The lowest energy mode has the greater strength of the two. This brings us back to the cause, alluded to in the previous section, of the kinks observed in *both* modes at $k\approx1.3$ Å^{-1} and then again at $k\approx1.6$ Å^{-1}. We can give two speculative reasons for this behavior. The first is that there may exist other modes that arise because of the substrate, and that these interfere slightly with the liquid modes. The most well known is the so-called flat modes that result from multiple scattering off the substrate-liquid system. In very thick films, this does not introduce any real complication; multiple scattering between the liquid roton excitation and the graphite Bragg peak produces a dispersionless ''flat'' mode with energy of roughly the roton gap energy and an intensity which is orders of magnitude less than the bulk mode. In thin films it remains unclear that multiple scattering modes should be as easily discernable from the liquid modes. Applying the same scaling factor of the strength of the bulk roton to the bulk flat mode, to the film modes, one would conclude that the flat mode should be insignificant in the films as well. If this scaling argument is correct then a second explanation is necessary. This comes from the theory. Careful inspection of Fig. 2 shows that there are three layer modes, with intensities varying with k and $\hbar\omega$. The lowest energy mode of this set, near $k\approx1.8$ Å^{-1} and $\hbar\omega\approx11$ K, is a layer roton that is propagating in the dense liquid layer at the solid-liquid interface. In this figure there remains sufficient scattering intensity in this mode to trace it back to lower k values. The important point is that this mode must level cross with the intermediate energy mode at $k\approx1.4$ Å^{-1} — approximately the same k where the kink is observed in the experimental modes. Thus, we speculate that the correct cause of the kinks in Fig. 10 is that layer modes must level cross with the intermediate-energy modes in this vicinity, similar to the theoretical prediction. If this remark is confirmed by future experiments with better energy resolution, then indeed the agreement between theory and experiment is impressive.

Finally, we comment on the quasibulk mode and the modes above the quasibulk roton. The three-phonon approximation yields a 3 K discrepancy between theory and experiment (for example, for the maxon). This energy difference is expected from the corresponding bulk calculations, done at this level of approximation. Adding more scattering processes will push the theoretical energy further down, thus reducing the discrepancy, but has little consequence otherwise. The addition of three-phonon processes lead to an enhanced scattering intensity between momentum in the range 1.4 Å$^{-1}\leqslant k\leqslant1.8$ Å^{-1}, and thus improve the agreement with experiment. It is interesting to note that in the accompanying theoretical paper[5] modes in that regime have spectral weight

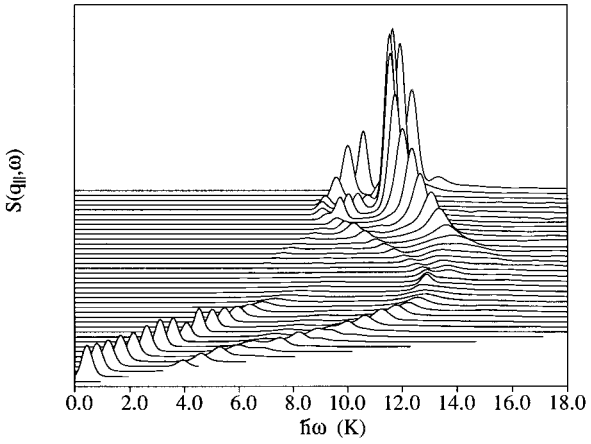

FIG. 11. Theoretical dynamic structure function, $S(q_\parallel,\omega)$, calculated with self-energy corrections to the three-phonon scattering processes.

that extends over the full thickness of the film, indicating their bulklike nature.

The solid curve in Fig. 2 also coincides well with a mode, between 0.4 Å$^{-1}\leqslant k\leqslant0.9$ Å^{-1}, but we see that this mode can be identified as a layered phonon. It is likely that as the film thickness continues to increase, this mode will evolve more and more to a bulk phonon.

Finally, we note that, mode for mode, there is quite good agreement between theory and experiment for momentum in the range 1.6 Å$^{-1}\leqslant k\leqslant2.0$ Å^{-1}. The obvious exception is that there are two experimental modes below the quasibulk roton. The lowest energy mode of the two has very low intensity, as can be seen from Figs. 7 and 8. We are led to three possible explanations. First, it is not a true mode in the sense that it will not survive at zero temperature. (Recall the discussion given in Sec. IV.) Second, this *is* the lowest energy layer roton that propagates in the high density first liquid layer. The next higher energy mode is either a second layer roton, but one that propagates in the next adjacent layer, or possibly even the ripplon. In either case it has an energy lower than that predicted by the the dynamical theory discussed here. According to the theory (Fig. 2), the next two higher energy modes are the ripplon and a layer mode, and have energies at approximately the quasibulk roton energy. The third explanation is that this is a true mode, but not of the type examined by the present theory. Indeed the vortex theories of Saarela[30] has predicted a mode with similar energy.

By looking at the results of our dynamical theory[5] that includes self-energy corrections to the three-phonon scattering processes, we can provide partial evidence that favors the second explanation. At the heart of the *scaled* CBF-BW approximation is the idea that further self-energy corrections can be incorporated into the CBF-BW framework by renormalizing the Feynman excitations. Technically, this was achieved by multiplying the Feynman excitations, that occur in the energy denominator of the CBF-BW expression, by a single scaling parameter which is adjusted to make the spectrum approximately agree with the experimental one in the bulk limit. In Fig. 11 we see directly from the dynamic structure function determined by this higher-order theory (same

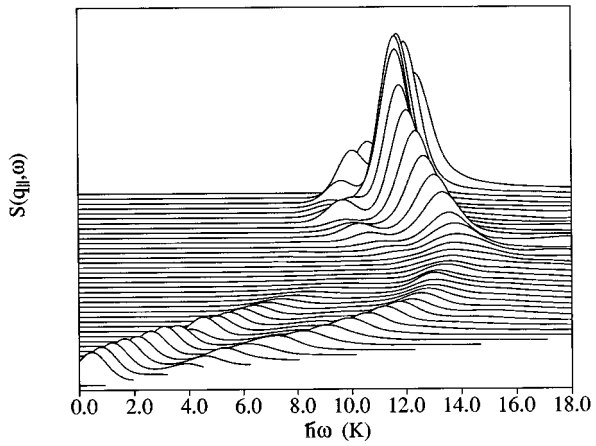

FIG. 12. Same as in Fig. 11, but with the modes broadend by convolving them with the experimental resolution function of 0.5 K width.

coverage) that now two modes have energy below the quasibulk roton. The lowest energy mode remains to be the layer roton that propagates in the first liquid layer, while the next higher energy mode is, in fact, the ripplon. Finally, it is instructive to convolve these modes with the experimental instrument resolution function; this has been done in Fig. 12. In doing so, we achieve a favorable comparison between the experimental (Fig. 3) and theoretical results.

VI. CONCLUSIONS

From our analysis of the experimental inelastic neutron-scattering data, plus guidance from our theoretical work, we have made significant progress in understanding the actual excitations occurring in real ^{4}He films. Our analysis supports the idea that a variety of modes exist, and that level crossings occur between them. We conclude that these results are extremely promising and have prompted new investigations using neutron scattering to help answer the remaining questions. Overall, the agreement between the experimental and theoretical excitations is very satisfying. The theory captures the detailed nature of the ripplon; the dispersion at low k, the fall off in intensity at intermediate k, and the level crossings at high k. The inclusion of three-phonon processes leads to an appreciably better agreement with experiment, over the Feynman theory, in the maxon-roton region of the forming bulklike excitation. At intermediate energies and momenta one finds modes in the experimental data which are in qualitative agreement with the theory. The accompanying paper gives the details of a multiphonon theory.[5] Besides giving a discussion of the three-phonon theory of the dynamic structure function, this work also involves incorporating yet higher-order scattering processes by effectively including higher-order self-energy corrections.

ACKNOWLEDGMENTS

This work was supported, in part, by the National Science Foundation under Grant Nos. PHY-9108066 and DMR-9509743 (to E.K.), by the BMFT Grant No. 03-LE3KON5 (to P.L.), by the North Atlantic Treaty Organization under Grant No. CRG 940127 (to E.K. and H.J.L.). B.E.C. and E.K. are grateful to the Institute Laue-Langevin, for partial support and for their kind hospitality. We are especially grateful to the kind hospitality of P. Nozíeres. Discussions with G. Agnolet, C. E. Campbell, P. Nozíeres, M. Saarela, and W. M. Saslow are gratefully acknowledged. Computational resources were provided by the Texas High Performance Computing Center.

*Present address: Los Alamos National Laboratory, Gp. T1, MS B221, Los Alamos, NM 87545.

†Present address: Department of Physics, Clark Atlanta University, J. P. Brawley Drive, Atlanta, GA 30314.

[1] G. Dash, Phys. Rep. **38**, 177 (1978).

[2] B. E. Clements, J. L. Epstein, E. Krotscheck, and M. Saarela, Phys. Rev. B **48**, 7450 (1993).

[3] M. Wagner and D. M. Ceperley, J. Low Temp. Phys. **94**, 185 (1994).

[4] H. J. Lauter, V. L. P. Frank, H. Godfrin, and P. Leiderer, in *Phase Transitions in Surface Films*, edited by H. Taub, G. Torzo, H. J. Lauter, and S. C. Fain, Jr. (Plenum Press, New York, 1991), Vol. 2, p. 135.

[5] B. E. Clements, E. Krotscheck, and C. J. Tymczak, following paper, Phys. Rev. B **53**, 12 253 (1996).

[6] P. A. Crowell and J. D. Reppy, Phys. Rev. Lett. **70**, 3291 (1993); Physica B **197**, 269 (1994).

[7] D. S. Greywall and P. A. Busch, Phys. Rev. Lett. **67**, 3535 (1991).

[8] C. G. Kuper, Physica **22**, 1291 (1956); **24**, 1009 (1956).

[9] H. J. Lauter, V. L. P. Frank, H. Godfrin, and P. Leiderer, in *Elementary Excitations in Quantum Fluids*, edited K. Ohbayashi and M. Watabe, Springer Series in Solid State Sciences Vol. 79 (Springer, Verlag, 1989), p. 99.

[10] H. Godfrin, V. L. P Frank, H. J. Lauter, and P. Leiderer, in *Phonons 89*, edited by S. Hunklinger, W. Ludwig, and G. Weiss (World Scientific, Singapore, 1989), p. 904.

[11] H. J. Lauter, H. Godfrin, V. L. P. Frank, and P. Leiderer, in *Excitations in Two-Dimensional and Three-Dimensional Quantum Fluids*, Vol. 257 of *NATO Advanced Study Institute, Series B: Physics*, edited by A. F. G. Wyatt and H. J. Lauter (Plenum, New York, 1991), p. 419.

[12] H. J. Lauter, H. Godfrin, and H. Wiechert, in *Proceedings of the Second International Conference on Phonon Physics*, edited by J. Kollàr, N. Kroo, M. Meynhard, and T. Siklos (World Scientific, Singapore, 1985), p. 842.

[13] E. Krotscheck, Phys. Rev. B **32**, 5713 (1985).

[14] G. Ji and M. Wortis, Phys. Rev. B **34**, 7704 (1986).

[15] J. L. Epstein and E. Krotscheck, Phys. Rev. B **37**, 1666 (1988).

[16] E. Krotscheck and C. J. Tymczak, in *Excitations in Two-Dimensional and Three-Dimensional Quantum Fluids*, Vol. 257 of *NATO Advanced Study Institute, Series B: Physics*, edited by A. F. G. Wyatt and H. J. Lauter (Plenum, New York, 1991), p. 257.

[17] E. Krotscheck and C. J. Tymczak, Phys. Rev. B **45**, 217 (1992).

[18] K. A. Gernoth and J. W. Clark, J. Low Temp. Phys. **96**, 153 (1994).

[19] B. E. Clements, E. Krotscheck, and M. Saarela, Z. Phys. B **94**, 115 (1994).

[20] B. E. Clements, J. L. Epstein, E. Krotscheck, M. Saarela, and C.

J. Tymczak, J. Low Temp. Phys. **89**, 585 (1992).
[21] L. Pricaupenko and J. Treiner, J. Low Temp. Phys. **96**, 19 (1994).
[22] B. E. Clements, H. Forbert, E. Krotscheck, H. J. Lauter, M. Saarela, and C. J. Tymczak, Phys. Rev. B **50**, 6958 (1994).
[23] B. E. Clements, E. Krotscheck, H. J. Lauter, and M. Saarela, in *Condensed Matter Theories*, edited by J. W. Clark, A. Sadiq, and K. A. Shoaib (Nova Science Publishers, Commack, New York, 1994), Vol. 9.
[24] B. E. Clements, H. Forbert, E. Krotscheck, and M. Saarela, J. Low Temp. Phys. **95**, 849 (1994).
[25] R. P. Feynman, Phys. Rev. **94**, 262 (1954).
[26] C. C. Chang and M. Cohen, Phys. Rev. B **11**, 1059 (1974).
[27] Papyex is a trademark of Carbon Lorraine, France.
[28] H. J. Lauter, H. P. Schildberg, H. Godfrin, H. Wiechert, and R. Haensel, Can. J. Phys. **65**, 1435 (1987), and references therein.
[29] H. W. Jackson, Phys. Rev. A **8**, 1529 (1973), and references therein.
[30] M. Saarela, B. E. Clements, E. Krotscheck, and F. V. Kusmartsev, J. Low Temp. Phys. **93**, 971 (1993).